Optical study of the orbital ordered state in $La_4Ru_2O_{10}$

2008 J. Phys.: Condens. Matter 20 325204

(http://iopscience.iop.org/0953-8984/20/32/325204)

J. Phys.: Condens. Matter **20** (2008) 325204 (5pp) doi:10.1088/0953-8984/20/32/325204

Optical study of the orbital ordered state in $La_4Ru_2O_{10}$

Dan Wu[1], P G Khalifah[2,3], D G Mandrus[4] and N L Wang[1,5]

[1] Beijing National Laboratory for Condensed Matter Physics, Institute of Physics, Chinese Academy of Sciences, Beijing 100080, People's Republic of China
[2] Department of Chemistry, Stony Brook University, Stony Brook, NY 11794, USA
[3] Department of Chemistry, Brookhaven National Laboratory, Upton, NY 11793, USA
[4] Materials Science and Technology Division, Oak Ridge National Laboratory, Oak Ridge, TN 37831, USA

E-mail: nlwang@aphy.iphy.ac.cn

Received 7 April 2008, in final form 20 June 2008
Published 9 July 2008
Online at stacks.iop.org/JPhysCM/20/325204

Abstract

We present the optical study of the ruthenate $La_4Ru_2O_{10}$, which undergoes a semiconductor–semiconductor transition at 160 K. Two Ru–Ru interband transition peaks can be found in its HT phase. When temperature decreases across the transition, a transfer of spectral weight from low to high energy occurs. The peak which is located at lower energy in the HT phase is strongly suppressed below 160 K. Based on the analysis of structural distortions associated with this transition, we show that the spectral changes can be well understood by considering energetically reasonable orbital-selective occupancies of Ru t_{2g} electrons. This proposed order of orbital energies offers specific insights into the HT insulating behavior, while the LT picture supports the current picture of a spin-singlet ground state.

(Some figures in this article are in colour only in the electronic version)

1. Introduction

The ruthenates, especially Sr_2RuO_4 and Ca_2RuO_4, have attracted much attention in the condensed matter community. Sr_2RuO_4 is a spin triplet superconductor with a T_c of about 1 K [1]. However, when Sr^{2+} is substituted by the smaller-size Ca^{2+}, the compound does not become more metallic; instead, it changes into an antiferromagnetic Mott insulator [2]. The contrasting physical properties between Sr_2RuO_4 and Ca_2RuO_4 have been intensively studied both theoretically and experimentally [3–5]. The insulating behavior of Ca_2RuO_4 is believed to be driven by a crystallographic distortion and a subsequent orbital ordering state of Ru 4d t_{2g} electrons [5–10]. In addition to Ca_2RuO_4, systematic studies on the orbital-selective Mott transition have been done on the isovalent substitution system $Ca_{2-x}Sr_xRuO_4$ with the range of $0 \leqslant x \leqslant 0.5$ [5, 11–15]. These studies focusing on the 4d t_{2g} orbital states have significantly advanced our knowledge on the orbital physics in transition metal oxides [16, 17].

Recently, a new ruthenate $La_4Ru_2O_{10}$, which like Ca_2RuO_4 has very distorted RuO_6 octahedra, was found experimentally [18]. $La_4Ru_2O_{10}$ has a semiconductor–semiconductor transition accompanied by a lowering of structural symmetry at $T_s = 160$ K. Its magnetic susceptibility undergoes a transition from Curie–Weiss behavior with $\mu_{eff} = 2.53\ \mu_B$ to a temperature-independent behavior with $\mu_{eff} = 0.38\ \mu_B$ when T decreases across T_s. This transition was originally hypothesized to be a result of quenching of local spin magnetic moment from $S = 1$ to 0, which was caused by the change from a triply degenerate Ru $t^3_{2g\uparrow}t^1_{2g\downarrow}$ (i.e. $d^2_{xy}d^1_{xz}d^1_{yz}$, $d^2_{xz}d^1_{xy}d^1_{yz}$, and $d^2_{yz}d^1_{xz}d^1_{xy}$) low-spin state to an $t^2_{2g\uparrow}t^2_{2g\downarrow}$ (i.e. $d^2_{xy}d^2_{xz}d^0_{yz}$) state [18]. However, in a later XAS study [19] and in band structure calculations [20], a very different nature of the phase transition was found. In those works, the spin state of each of the two inequivalent Ru^{4+} sites present at low temperature (LT), Ru1 and Ru2, was shown to remain $S = 1$ below 160 K, and both have the specific $d^1_{xy}d^2_{xz}d^1_{yz}$ orbital population (where x is defined to be in the direction of the long Ru–O bonds, and y is along the short Ru–O bonds). Considering the low-T magnetic properties of $La_4Ru_2O_{10}$, the spin-singlet dimer formation driven by the orbital ordering was suggested for the phase transition at T_s. Furthermore, a very recent polarized optical

[5] Author to whom any correspondence should be addressed.

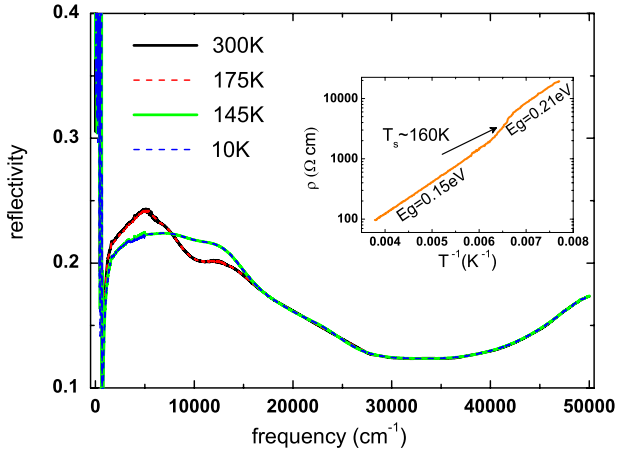

Figure 1. The *bc*-plane reflectivity $R(\omega)$ of $La_4Ru_2O_{10}$ at four different temperatures in the range of 30–50 000 cm^{-1}. The inset shows the dc resistivity as a function of temperature. An obvious increase of resistivity occurs at ∼160 K. The energy gap increases from 0.15 to 0.21 eV when T crosses T_s.

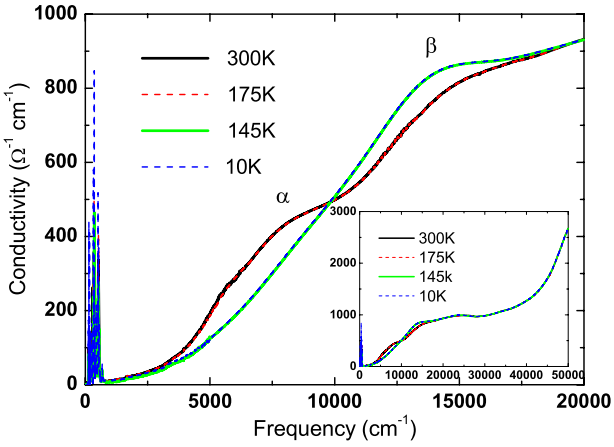

Figure 2. Optical conductivity spectrum of $La_4Ru_2O_{10}$ from 30 to 20 000 cm^{-1} at four different temperatures measured in the *bc*-plane. Two prominent peaks labeled as α and β are present in the HT optical conductivity spectra. When T is lowered below T_s, the α peak is obviously suppressed, and the spectral weight transferred to higher energy enhances the β peak in the LT phase. The inset shows the full optical conductivity spectrum of $La_4Ru_2O_{10}$ over the entire accessible measurement range (30–50 000 cm^{-1}).

measurement showed a strongly anisotropic optical response in the LT phase, giving additional strong experimental evidence for the formation of a spin-singlet state in LT $La_4Ru_2O_{10}$ [21].

Although a number of studies, including the polarized optical study [21], have been performed on $La_4Ru_2O_{10}$, some important issues regarding the mechanism and driving force for this unusual phase transition remain unclear. In particular, there is still an axial anisotropy in the Ru–O bond lengths of each individual RuO_6 octahedron in the high temperature (HT) structure, but with the direction of the long axis alternating between x and y, in contrast to the LT structure, where the long axis always points along x. Motivated by this, we further investigated the optical response across the transition. Two Ru–Ru interband transition peaks were found in the HT phase. As the temperature decreases across T_s, there is spectral weight transfer from the lower energy peak to the higher energy peak. As we will discuss below in detail, on the basis of structural distortions for the HT and LT phases, the spectral changes can be well understood from a specific shift in the orbital-selective occupancies of Ru t_{2g} electrons, offering new insights into the HT insulating state.

2. Experiment

The $La_4Ru_2O_{10}$ single crystals were grown by a floating zone method [19]. A crystal with a cleaved surface (*bc*-plane) with an area about $5\times3\times1$ mm^3 was used for optical measurements. The frequency-dependent reflectance spectra $R(\omega)$ at four different temperatures were measured by a Bruker IFS 66 v/s spectrometer in the range from 30 to 25 000 cm^{-1} and a home-made grating spectrometer from 25 000 to 50 000 cm^{-1}. The sample was mounted on an optically black cone in a cold-finger flow cryostat. An *in situ* gold (30–15 000 cm^{-1}) and aluminum (9000–50 000 cm^{-1}) overcoating technique was employed for reflectance measurements. The Kramers–Kronig transformation of $R(\omega)$ was used to obtain the optical conductivity spectra. Constant values were used for both low frequency and high frequency extrapolations. For the high frequency side, a function of ω^{-4} was used above the constant extrapolation up to 400 000 cm^{-1}.

Figure 1 displays the T-dependent reflectance spectra in the range of 30–50 000 cm^{-1}. The reflectance of the sample is rather low (about 0.2) in a very wide frequency range for both the high temperature (HT) and low temperature (LT) phases, indicating semiconducting behavior of $La_4Ru_2O_{10}$ at all temperatures studied. There is little temperature dependence for the reflectance in either of the two semiconducting phases. Nevertheless, a distinct change of the reflectance spectra when T crosses T_s can be clearly seen. As shown in figure 1, the reflectance in the frequency range of 800–8000 cm^{-1} decreases somewhat when T goes through 160 K; however, it increases a little in the range of 8000–15 000 cm^{-1} below T_s. Above 15 000 cm^{-1}, the reflectance does not change with T. In the inset of figure 1, we show the dc resistivity as a function of T^{-1} for the same crystal. An obvious increase of resistivity occurs at ∼160 K. From the dc resistivity data, we obtain two distinctly different activated gaps of 0.15 eV (LT) and 0.21 eV (HT).

The optical conductivity spectra in the frequency range from 30 to 20 000 cm^{-1} are shown in figure 2. The sharp peaks between 100 and 600 cm^{-1} are due to optical phonons. If we remove the phonon contribution, the optical conductivity of the sample is very low in the low frequency region (below 2000 cm^{-1}). The absence of the free-carrier Drude component at these low frequencies is in accord with the presence of a semiconducting band gap in this material. With increasing ω, the conductivity in HT and LT phases begins to increase rapidly. Two obvious peaks are found in the HT phase, centered at about 7000 cm^{-1} (α) and 14 000 cm^{-1} (β). Below 160 K, the spectral weight transfers somewhat from low to high energy, leading the α peak to be noticeably suppressed. This transferred spectral weight also makes the β

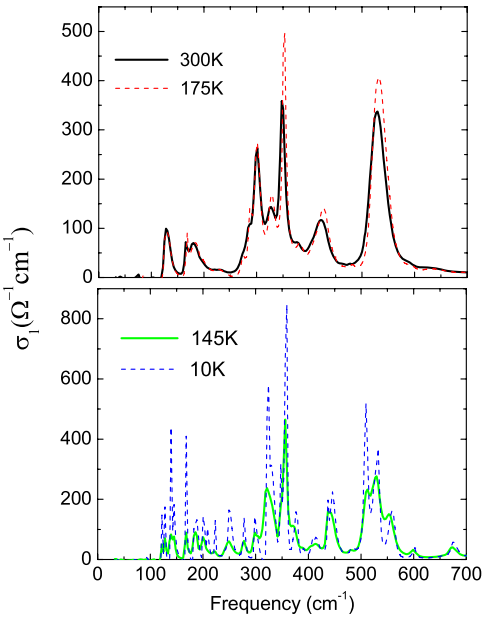

Figure 3. Expanded plot of the low frequency region of the *bc*-plane optical conductivity spectra. Different series of phonon modes can be found in HT (upper panel) and LT (lower panel) phases.

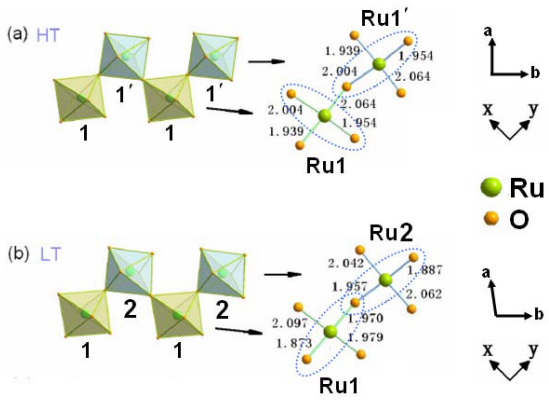

Figure 4. (a) The arrangement of RuO_6 octahedra in the *ab*-plane of HT $La_4Ru_2O_{10}$ with the two classes of orbitally distinct ruthenium sites (Ru1, Ru1′) labeled. (b) The arrangement of RuO_6 octahedra in the *ab*-plane of LT $La_4Ru_2O_{10}$ with the two classes of symmetrically distinct ruthenium sites (Ru1, Ru2) labeled. In both panels, the lengths (Å) of Ru–O bonds in the *ab*-plane are indicated and the compressed Ru–O bonds are circled.

peak become stronger in the LT phase. The inset of figure 2 gives the optical conductivity spectra in the full measured range (30–50 000 cm^{-1}). The rapid increasing of $\sigma(\omega)$ above 30 000 cm^{-1} must be due to interband transition between O 2p and Ru e_g states, while the very weak peak between 20 000 and 30 000 cm^{-1} must come from the transition between O 2p and Ru t_{2g} states.

The structural transition also causes very distinct changes in the phonon structure of $La_4Ru_2O_{10}$. In figure 3, we show the optical conductivity spectra in the low frequency range from 30 to 700 cm^{-1}. Due to the low (monoclinic) lattice symmetry of HT $La_4Ru_2O_{10}$, many phonon modes are present in the HT spectra. On cooling below T_s, there is clear splitting of many modes as well as appearance of a number of new phonon modes. These characteristics reflect the lowering of the lattice symmetry (to triclinic) on cooling below the structural transition.

3. Discussion

It is very important to fully understand the interband transition peaks in the optical conductivity spectra. As discussed above, the very high energy spectral features can be readily ascribed to interband transition between O 2p and Ru 4d bands, in accord with prior band structure calculations [19, 20]. The key issue is therefore to understand the origin of the two low energy peaks of α and β in the HT phase and the associated spectral weight transfer that occurs on crossing T_s. Based on the energy and behavior of the α and β peaks, they should be assigned to d–d interband transitions (or intersite electron hopping between two neighboring Ru sites), which are only allowed because of the mixing or hybridization between Ru t_{2g} and O 2p bands. They are directly associated with the orbital occupancies in the t_{2g} states, and will thus provide critical information for elucidating the orbital occupancy of LT and HT $La_4Ru_2O_{10}$.

The orbital occupancies of $La_4Ru_2O_{10}$ are closely tied to structural features, as any increase in a d-orbital occupancy will lead to additional electrostatic repulsions with oxygen atoms between the lobes of the d orbital, and a concomitant elongation of these Ru–O bonds. Equivalently, shortened Ru–O bonds reflect decreased orbital occupancies. For consistency, the Cartesian axes in HT $La_4Ru_2O_{10}$ are defined in the same crystallographic sense as those in LT $La_4Ru_2O_{10}$, with the x axis in the $+a-b$ direction, the y axis in the $+a+b$ direction, and the z axis in the $+c$ direction. The RuO_6 octahedra do not have perfect octahedral symmetry, so all six Ru–O bonds in a given octahedron have different lengths and they are imperfectly aligned with the Cartesian axes [18, 22, 23].

In the case of HT $La_4Ru_2O_{10}$, it is extremely important to note that while all of the Ru sites are symmetrically equivalent, this does not constrain all three of their t_{2g} d orbitals to have identical energies. Furthermore, and much more subtly, it does not constrain symmetry-related orbitals in pairs of Ru atoms to have identical orientations relative to the crystallographic axes. In HT $La_4Ru_2O_{10}$, the $P2_1/c$ symmetry results in two possible variants of the single Ru crystallographic site, which we will refer to as Ru1 and Ru1′. The orbital symmetry alternates with respect to the crystallographic axes such that all four nearest neighbor sites for every Ru1 are Ru1′ sites. This includes both the two nearest neighbors in the *ab* crystallographic plane (along the zigzag direction, shown in figure 4(a)), and the two nearest neighbors in the *c*-direction (along infinite corner-sharing chains, not shown). Similarly, each Ru1′ site has only Ru1 nearest neighbors. The monoclinic symmetry dictates that nearest neighbor octahedra (*always* one Ru1 and one Ru1′) must have d_{xy} orbitals with identical energies, but with the energies of the d_{xz} and d_{yz} states flipped between the neighbors (illustrated schematically in figure 5(a)). This means that the Ru1 d_{xz} orbitals are identical in energy to the d_{yz} orbitals of the

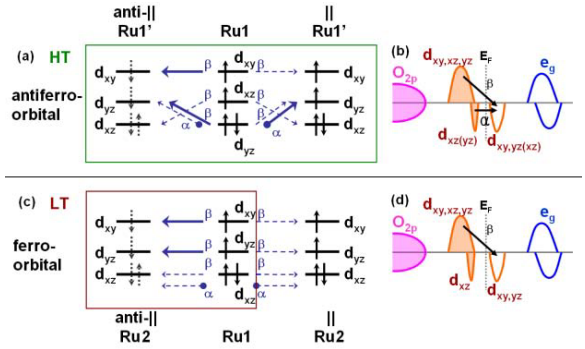

Figure 5. Schematic distribution of orbital energies for the Ru 4d t_{2g} orbitals in HT and LT $La_4Ru_2O_{10}$. The microscopic configurations are diagrammed for neighboring sites ((a) and (c)), since the transitions cannot be understood by just considering the overall density of states ((b) and (d)). (a) Neighboring Ru ions in the HT phase have two possible configurations, parallel spins or antiparallel spins, that occur with approximately equal probabilities. In the parallel case (right), only the Ru1 α transition ($d_{xz}\downarrow$–$d_{xz}\downarrow$) is allowed. In the antiparallel case (left), only the Ru1 β transitions ($d_{xy}\uparrow$–$d_{xy}\uparrow$ and $d_{yz}\uparrow$–$d_{yz}\uparrow$) are allowed. Therefore, both α and β transitions are observed in the HT optical conductivity spectra (figure 2). Bold arrows indicate allowed transitions while narrow dashed arrows indicate forbidden transitions. (b) Schematic distribution of orbital energies with arrows indicating the two spectroscopically observed interband transition between HT Ru t_{2g} levels (α and β). Alternative labels for the Ru1′ sites are given in parentheses. (c) In the LT phase, the 100% antiparallel arrangement (left) allows only β transitions ($d_{xy}\uparrow$–$d_{xy}\uparrow$ and $d_{yz}\uparrow$–$d_{yz}\uparrow$). The α transition is forbidden for reasons of both spin and occupancy (d_{xz} levels are fully occupied in both Ru1 and Ru2), and is absent in the measured LT optical conductivity (figure 2). Since all neighboring octahedra have antiparallel spin arrangements, the possible parallel transitions (right) are not relevant to this system. (d) Schematic distribution of orbital energies in LT $La_4Ru_2O_{10}$, with an arrow indicating the one allowed type of transition (β).

Ru1′ orbitals, and that the Ru1 d_{yz} and Ru1′ d_{xz} orbitals also have identical energies.

In HT $La_4Ru_2O_{10}$, the two bonds which lie along the $z(c)$-direction are somewhat longer than the other four, which lie in the xy-plane (ab-plane), which indicates a relative compression of Ru–O bonds in the xy-plane. In this case, the d_{xy} orbital is expected to have the highest energy level of t_{2g} orbitals because of the maximized Coulombic repulsions between the lobes of the d_{xy} orbital and the four oxygen atoms in the xy-plane. As shown in figure 4(a), the two Ru1–O bonds lying along the y-direction are longer than the two along the x-direction, but are shorter in the neighboring Ru1′O_6 octahedra. As a result, the d_{yz} orbital will be pushed to a lower energy than the d_{xz} orbital in Ru1O_6 octahedra, while conversely the d_{xz} level is lower in energy in Ru1′O_6 octahedra. Based on these alternating energies, we propose the schematic energy level diagram for the HT Ru t_{2g} orbitals in figure 5(a). In this scheme, the d_{xz} and d_{yz} levels will alternatively become the lowest energy t_{2g} level and be doubly occupied, and both the d_{xz} and d_{yz} levels will always be lower in energy than the d_{xy} level.

Now let us analyze the permitted interband transitions for the system. The dominant contribution to optical conductivity arises from electric dipole (**p**) transitions. The d–d transition becomes allowed by mixing with oxygen 2p orbitals in a manner such as d $\rightarrow$ O2p $\rightarrow$ d, giving non-zero matrix element for $\langle d_{final}|\mathbf{p}|O_{2p}\rangle\langle O_{2p}|\mathbf{p}|d_{initial}\rangle$. Considering the orthorhombic character of t_{2g} orbitals, the effective d–d transition should occur between suborbitals of the same type. Additionally, the transition must maintain the same spin polarization (since spin flips are forbidden for optical transition). Since HT $La_4Ru_2O_{10}$ has a Curie–Weiss magnetic susceptibility, its Ru ions must possess local moments but lack long-range magnetic order. In this case, there are two possible spin moment configurations for the neighboring Ru ions: parallel spins or antiparallel spins. As shown in figure 5(a), when the neighboring Ru ions have parallel spin moments, only the minority spin $d_{yz}\downarrow$ electron is allowed to hop from a Ru1 site to neighboring Ru1′ sites, while the majority spin $d_{xz}\uparrow$, $d_{yz}\uparrow$, and $d_{xy}\uparrow$ electrons are forbidden to hop due to the Pauli exclusion principle and the impossibility of spin-flip transitions (here 'minority' and 'majority' refer to the configuration of a single ion, since long-range order is not present). In the antiparallel case, more orbitals are accessible to electrons hopping from Ru1 sites, and both $d_{xy}\uparrow$–$d_{xy}\uparrow$ and $d_{xz}\uparrow$–$d_{xz}\uparrow$ transitions from majority spin states may happen, though the $d_{yz}\uparrow$–$d_{yz}\uparrow$ is forbidden due to the doubly occupied Ru1′d_{yz} target level, and the minority spin $d_{xz}\downarrow$–$d_{xz}\downarrow$ transition is forbidden for both spin and occupancy reasons.

When we consider the relative energies of the different t_{2g} d orbitals, we can elucidate the origin of the two experimentally observed sets of transitions (α and β) in HT $La_4Ru_2O_{10}$, as shown in figure 5(b). The α peak corresponds to the lower energy minority spin transitions out of the doubly occupied Ru1 t_{2g} orbital, $d_{yz}\downarrow$–$d_{yz}\downarrow$, and into a parallel spin neighbor. The higher energy β transition includes both $d_{xy}\uparrow$–$d_{xy}\uparrow$ and $d_{xz}\uparrow$–$d_{xz}\uparrow$ transitions from Ru1 to an antiparallel spin neighbor. Since the Ru1 and Ru1′ sites are symmetrically equivalent, identical energy transitions will occur out of the Ru1′ sites, but with a transposition of the d_{xz} and d_{yz} orbital labels. Even though $La_4Ru_2O_{10}$ has relatively strong spin coupling between neighboring sites ($\theta = -71$ K, [18]), there should be nearly identical populations of parallel and antiparallel neighboring spins in the HT phase. It should be noted that if the relative energies of the different t_{2g} orbitals are small relative to the band widths and it is therefore impossible to assign double occupancy to just one of the three t_{2g} orbitals, the nature of the observed transitions will not substantially change, since the spin selection rules (and not the orbital occupancies) play the dominant role in determining the observed transitions of HT $La_4Ru_2O_{10}$.

When T drops below 160 K, the first order structural transition from monoclinic ($P2_1/c$) to triclinic ($P\bar{1}$) symmetry of $La_4Ru_2O_{10}$ occurs and leads to both larger magnitude and more cooperative distortions of the Ru–O octahedra. In the lower symmetry space group of LT $La_4Ru_2O_{10}$, there are two symmetrically inequivalent octahedral Ru sites, Ru1 and Ru2, with entirely different sets of Ru–O bond lengths, as shown in figure 4(b). The orbitally ordered state is reflected in the very large variations of Ru–O bond lengths, which differ by roughly 0.10 Å between the shortest and longest bonds.

The cooperative nature of the transition is apparent in the coalignment of bonds of similar lengths, indicative of ferro-orbital ordering. The four strongly elongated Ru–O bonds lie in the x direction, while the four severely compressed Ru–O have a y orientation. Since the d_{xz} orbital is the only t_{2g} d orbital to avoid compression, it becomes the lowest energy t_{2g} state and is doubly occupied in $La_4Ru_2O_{10}$, a result confirmed by band structure calculations [19, 20]. The other two t_{2g} d orbitals (d_{xy} and d_{yz}) are very close in energy, with a separation of only 0.05 eV [20]. Since this is much smaller than the Hund's rule coupling energy, the two residual Ru 4d electrons will singly occupy the d_{xy} and d_{yz} orbitals respectively, and collectively lead to an orbitally ordered state with an $S = 1$ electron configuration of $d^2_{xz}d^1_{xy}d^1_{yz}$ for both the Ru1 and Ru2 sites. In this LT ferro-orbitally ordered state, the minority spin α transition will be completely suppressed since now all (and not just half of) the Ru sites have doubly occupied d_{xz} orbitals.

The macroscopic low temperature quenching of the total magnetic moment of $La_4Ru_2O_{10}$ reflects the extremely robust antiparallel spin arrangements resulting from the Ru1–Ru2 spin dimer formation. This antiparallel arrangement means that the α transition is spin forbidden, and is expected to disappear in any antiparallel spin state (including an antiferromagnetically ordered state), whether or not orbital order (which makes the transition occupancy forbidden) is present. This is clearly reflected in the suppression of the α peak in the measured optical conductivity spectra (figure 2), and is wholly consistent with the previously proposed $d^2_{xz}d^1_{xy}d^1_{yz}$ orbitally ordered state. The fully antiparallel spin arrangement of LT $La_4Ru_2O_{10}$ is also directly responsible for the enhancement of the β transition, since the β transition will now be allowed for all pairs of Ru octahedra, and not just half as was the case for spin-disordered HT $La_4Ru_2O_{10}$.

To summarize, we have studied the interband transitions in optical conductivity spectra of the ruthenate $La_4Ru_2O_{10}$, which undergoes an abrupt magnetic transition at 160 K. We found two Ru–Ru interband transitions in the HT phase, but only one interband transition in the LT phase. The spectral weight of the interband transition at lower energy is transferred to higher energy as the temperature decreases across T_s, for reasons associated with the different magnetic states on each side of the transition. Taking structural features into consideration, we suggest that the orbital ordering of Ru t_{2g} levels may have already occurred in the HT phase, leading to the release of the Ru t_{2g} orbital degeneracy. On the basis of orbital-selective occupancy in different Ru sites for both two phases, we demonstrate that the spectral change can be well understood by considering changes in the orbital-selective occupancies of Ru t_{2g} electrons. On the other hand, the LT optical conductivity spectra are entirely consistent with the picture of spin dimer formation in the low temperature phase [19–21]. Our proposed orbital ordering pictures for the HT and LT regimes provide a natural explanation for the phase transition of $La_4Ru_2O_{10}$.

Acknowledgments

We acknowledge Z Fang and Hua Wu for helpful discussions. This work is supported by the National Science Foundation of China, the Knowledge Innovation Project of the Chinese Academy of Sciences, and the 973 project of the Ministry of Science and Technology of China. The work at ORNL was sponsored by the US Department of Energy under contract No DE-AC05-00OR22725 with the Oak Ridge National Laboratory, managed by UT-Battelle, LLC.

References

[1] Maeno Y, Hashimoto H, Yoshida K, Nishizaki S, Fujita T, Bednorz J G and Lichtenberg F 1994 *Nature* **372** 532
[2] Nakatsuji S, Ikeda S and Maeno Y 1997 *J. Phys. Soc. Japan* **66** 1868
[3] Woods L M 2000 *Phys. Rev.* B **62** 7833
[4] Tran T T, Mizokawa T, Nakatsuji S, Fukazawa H and Maeno Y 2004 *Phys. Rev.* B **70** 153106
[5] Anisimov V I, Nekrasov I A, Kondakov D E, Rice T M and Sigrist M 2000 *Eur. Phys. J.* B **25** 191
[6] Cao G, McCall S, Shepard M, Crow J E and Guertin R P 1997 *Phys. Rev.* B **56** R2916
[7] Mizokawa T, Tjeng L H, Saweatzky G A, Ghiringhelli G, Tjernberg O, Brookers N B, Fukazawa H, Nakatsuji S and Maeno Y 2001 *Phys. Rev. Lett.* **87** 077202
[8] Jung J H, Fang Z, He J P, Kaneko Y, Okimoto Y and Tokura Y 2003 *Phys. Rev. Lett.* **91** 056403
[9] Zegkinoglou I, Strempfer J, Nelson C S, Hill J P, Chakhalian J, Bernhard C, Lang J C, Srajer G, Fukazawa H, Nakatsuji S, Maeno Y and Keimer B 2005 *Phys. Rev. Lett.* **95** 136401
[10] Jung J H 2004 *Solid State Commun.* **133** 103
[11] Nakatsuji S and Maeno Y 2000 *Phys. Rev. Lett.* **84** 2666
[12] Kurokawa M and Mizokawa T 2002 *Phys. Rev.* B **66** 024434
[13] Lee J S, Lee Y S, Noh T W, Oh S-J, Yu J, Nakatsuji S, Fukazawa H and Maeno Y 2002 *Phys. Rev. Lett.* **89** 257402
[14] Fang Z, Nagaosa N and Terakura K 2004 *Phys. Rev.* B **69** 045116
[15] Mizokawa T, Tjeng L H, Lin H-J, Chen C T, Schuppler S, Nakatsuji S, Fukazawa H and Maeno Y 2004 *Phys. Rev.* B **69** 132410
[16] Jeng H-T, Lin S-H and Hsue C-S 2006 *Phys. Rev. Lett.* **97** 067002
[17] Lee J S, Moon S J, Yang B J, Yu J, Schade U, Yoshida Y, Ikeda S-I and Noh T W 2007 *Phys. Rev. Lett.* **98** 097403
[18] Khalifah P, Osborn R, Huang Q, Zandbergen H W, Jin R, Liu Y, Mandrus D and Cava R J 2002 *Science* **297** 2237
[19] Wu H, Wu Z, Burnus T, Denlinger J D, Khalifah P G, Mandrus D G, Jang L-Y, Hsieh H H, Tanaka A, Liang K S, Allen J W, Cava R J, Khomskii D I and Tjeng L H 2006 *Phys. Rev. Lett.* **96** 256402
[20] Eyert V, Ebbinghaus S G and Kopp T 2006 *Phys. Rev. Lett.* **96** 256401
[21] Moon S J, Choi W S, Kim S J, Lee Y S, Khalifah P G, Mandrus D and Noh T W 2008 *Phys. Rev. Lett.* **100** 116404
[22] Boullay P, Mercurio D, Bencan A, Meden A, Drazic G and Kosec M 2003 *J. Solid State Chem.* **170** 294
[23] Ebbinghaus S G 2005 *Acta Crystallogr.* C **61** i96